eLIFE elifesciences.org

RESEARCH ARTICLE

Figures and figure supplements

Arabidopsis heterotrimeric G proteins regulate immunity by directly coupling to the FLS2 receptor

Xiangxiu Liang *et al*

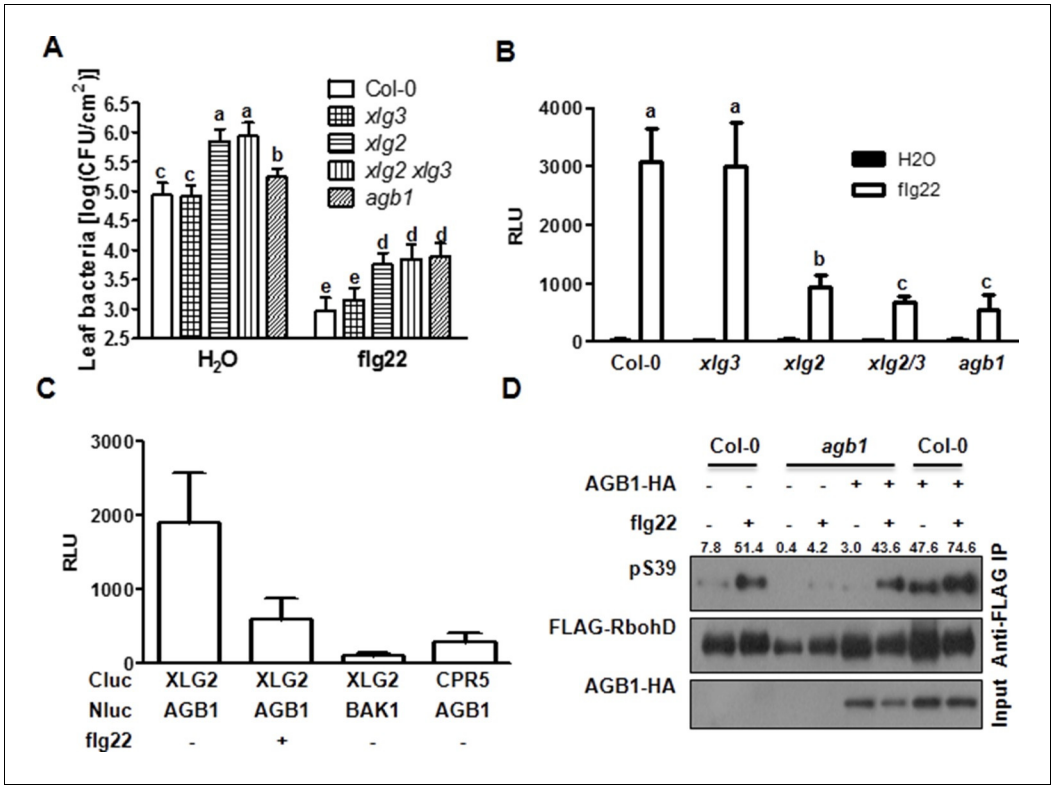

Figure 1. G proteins are required for FLS2-mediated immunity. (**A**) *XLG2/3* and *AGB1* play overlapping but not identical roles in disease resistance to *Pst*. Plants of indicated genotypes were infiltrated with H_2O and flg22 1 day before infiltration with *P. syringae* DC3000, and bacteria number was determined 2 days later (mean ± SD; $n \geq 6$; $p<0.05$, Student's t-test; different letters indicate significant difference). (**B**) *xlg2/3* and *agb1* are similarly compromised in flg22-induced ROS burst. Leaves of the indicated genotypes were examined for flg22-induced ROS production, and peak RLU values are shown (mean ± SD; $n \geq 6$; $p<0.05$, Student's t-test; different letters indicate significant difference). (**C**) Flg22 treatment disrupts XLG2-AGB1 interaction. Cluc-XLG2 and AGB1-HA-Nluc constructs are transiently expressed in *Nb* leaves, relative luminescence unit (RLU) was measured 2 days later. Cluc-CPR5 and BAK1-HA-Nluc were used as negative control (mean ± SD; $n \geq 6$). (**D**) Flg22-induced RbohD phosphorylation is impaired in *agb1*. FLAG-RbohD and/or AGB1-HA constructs were expressed under control of the 35S promoter in WT or *agb1* protoplasts. The FLAG-RbohD protein was affinity purified and subject to anti-FLAG and anti-pSer39 immunoblot analyses. Numbers indicate arbitrary units of RbohD pS39 phosphorylation calculated from densitometry measurements normalized to total FLAG-RbohD protein. Each experiment was repeated three times, and data of one representative experiment are shown.

DOI: 10.7554/eLife.13568.003

The following source data is available for figure 1:

Source data 1. Raw data and exact p value of ***Figure 1A***, ***B*** and ***Figure 1—figure supplement 1***.

DOI: 10.7554/eLife.13568.004

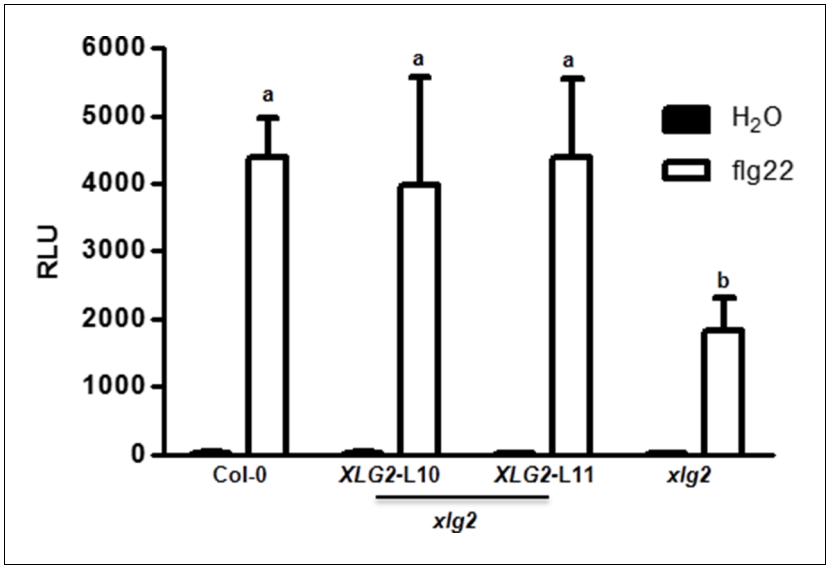

Figure 1—figure supplement 1. Flg22-induced ROS burst is compromised in *xlg2* plants. Flg22-induced ROS burst is compromised in *xlg2* plants. Col-0, *xlg2,* and *xlg2* transgenic lines complemented with the *XLG2* transgene under control of the *XLG2* native promoter were examined for flg22-induced ROS burst. RLU represent peak value of ROS production after flg22 treatment (mean ± SD; n ≥ 6; representative data from three independent experiments are shown).

DOI: 10.7554/eLife.13568.005

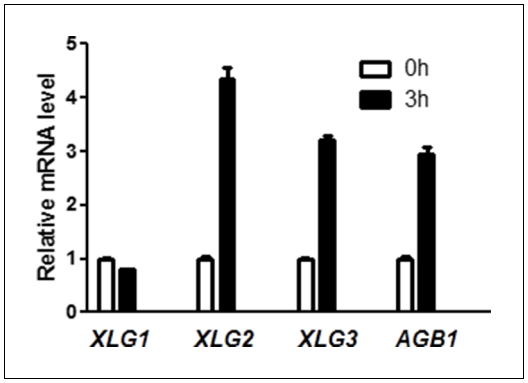

Figure 1—figure supplement 2. *XLG2/3* and *AGB1*, but not *XLG1*, are transcriptionally induced by flg22. qRT-PCR analyses of the indicated genes in WT plants 0 hr and 3 hr after infiltration with flg22. Representative data from three independent experiments are shown.
DOI: 10.7554/eLife.13568.006

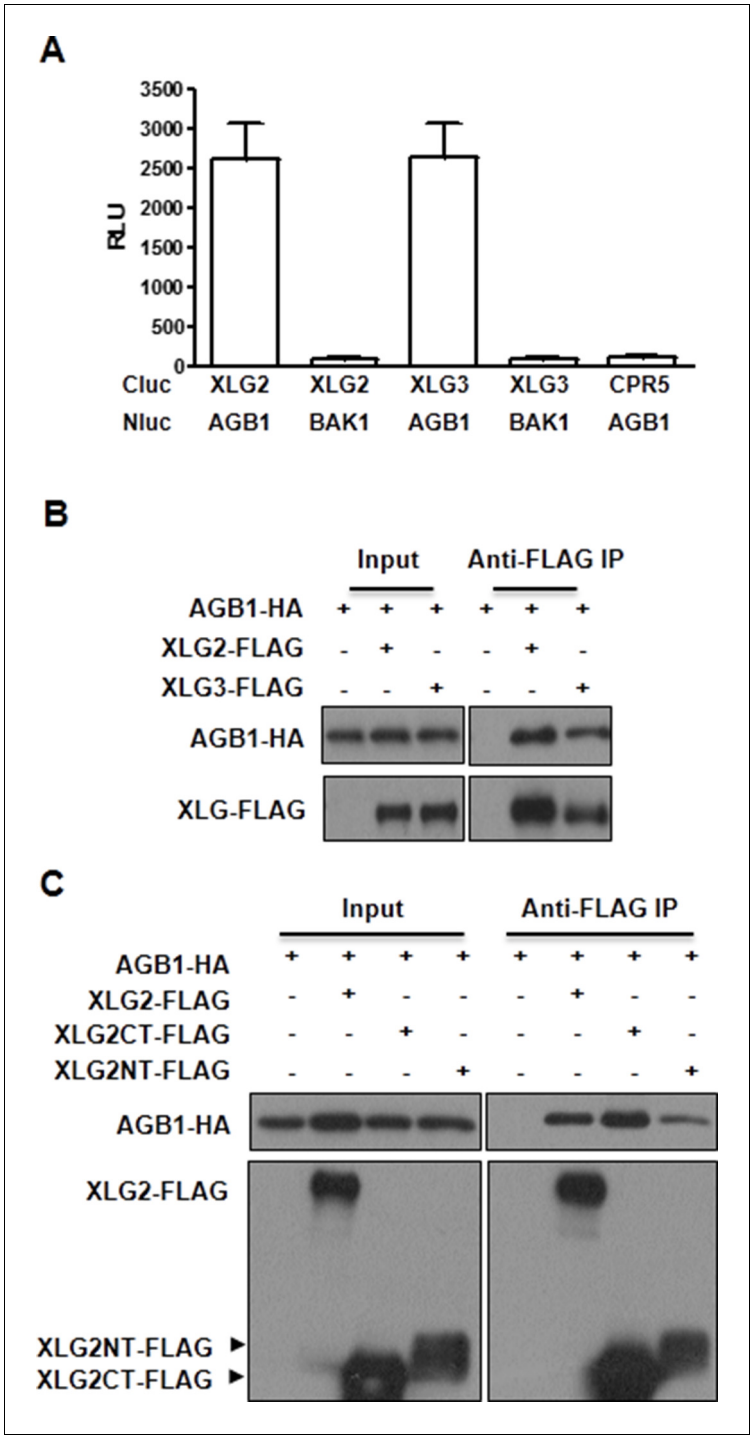

Figure 1—figure supplement 3. XLG2/3 interact with AGB1 through both N and C termini. (**A**) Luciferase complementation assay for XLG2/3-AGB1 interactions in *Nb* plants. *Nb* leaves were infiltrated with *Agrobacterium tumefaciens* strains carrying the indicated constructs and luciferase activity was recorded 2 days later (mean ± SD; n≥6; representative data from three independent experiments are shown). (**B**) Co-IP assay for XLG2/3-AGB1 interaction in protoplasts. Three independent experiments were performed with similar results. (**C**) Both N and C termini of XLG2 interact with AGB1. XLG2NT-FLAG contains amino acids 1–458 whereas XLG2CT-FLAG contains amino acids 459–861. The indicated constructs were expressed in WT protoplasts, immunoprecipitated with agarose-conjugated FLAG antibody, and the immune complex was subject to immunoblot with specific antibodies.

DOI: 10.7554/eLife.13568.007

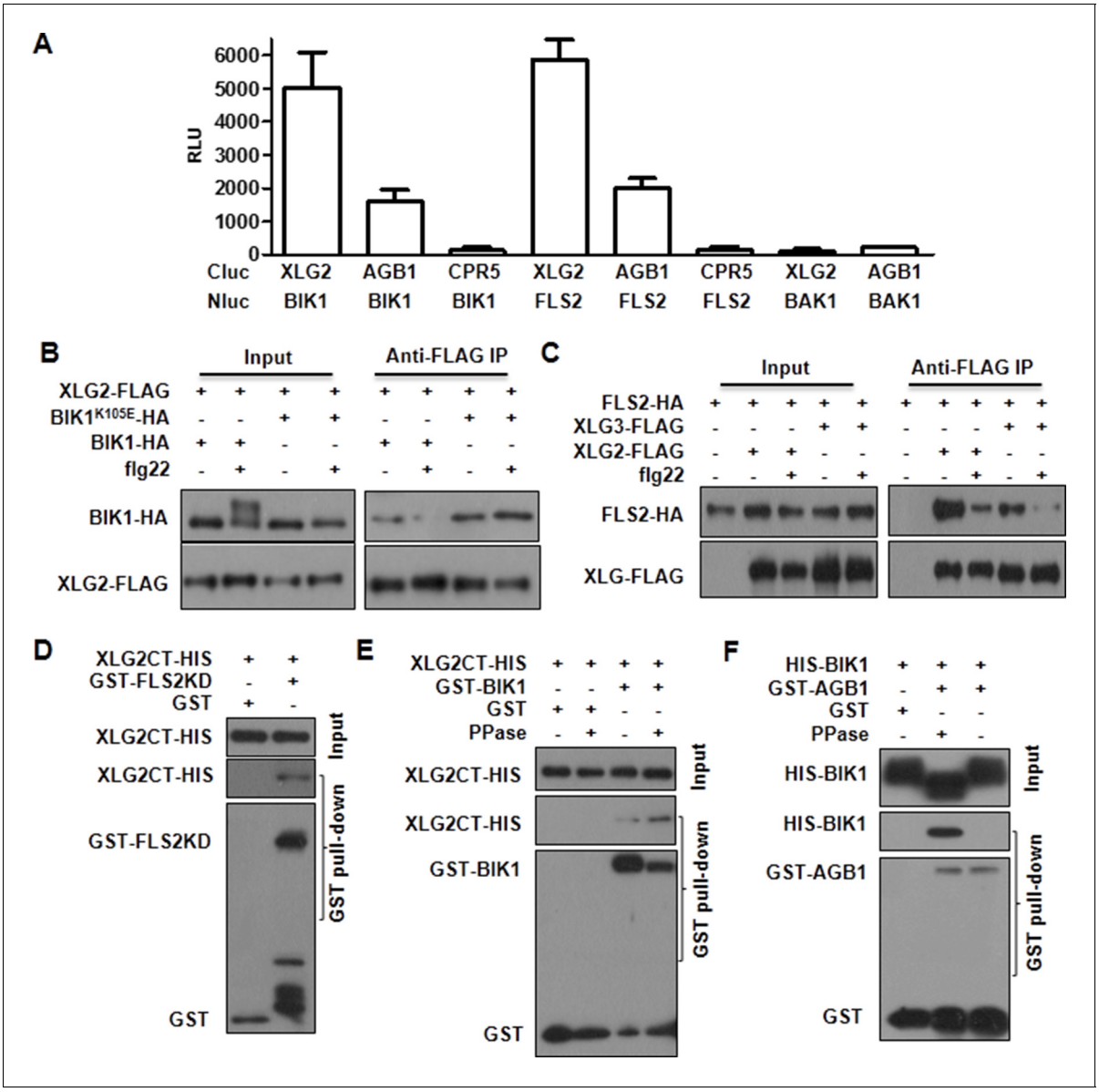

Figure 2. Flg22 regulates interactions between G proteins and the FLS2-BIK1 receptor complex. (**A**) XLG2 and AGB1 interact with BIK1 and FLS2 in *Nb* plants. The indicated Nluc and Cluc constructs were transiently expressed in *Nb* plants for luciferase complementation assay. Relative luminescence unit (RLU) shows the strength of protein-protein interaction (mean ± SD; $n \geq 6$. (**B**) XLG2 interacts with BIK1 in Arabidopsis protoplasts and the interaction is dynamically regulated by flg22. (**C**) XLG2/3 interact with FLS2 in Arabidopsis protoplasts and the interaction is dynamically regulated by flg22. The indicated constructs were co-expressed in WT protoplasts, and Co-IP assays were performed using agarose-conjugated anti-FLAG antibody. $BIK1^{K105E}$ carries a mutation in the ATP-binding site. (**D**) The C terminus of XLG2 directly interacts with FLS2 kinase domain. XLG2CT-HIS (amino acids 459–861) was incubated with GST or GST-FLS2KD (FLS2 kinase domain) for GST pull-down assay and detected by anti-HIS and anti-GST immunoblots. (**E**) XLG2 primarily interacts with non-phosphorylated BIK1. XLG2CT-HIS was incubated with GST or GST-BIK1 that was untreated or pre-treated with λ phosphatase (PPase), and GST pull-down assay was performed. (**F**) AGB1 interacts with the non-phosphorylated BIK1. Untreated or PPase-treated BIK1-HIS was incubated with GST or GST-AGB1, and GST pull-down assay was performed. Each experiment was repeated two (**D–F**) or three (**A–C**) times, and data of one representative experiment are shown.

DOI: 10.7554/eLife.13568.008

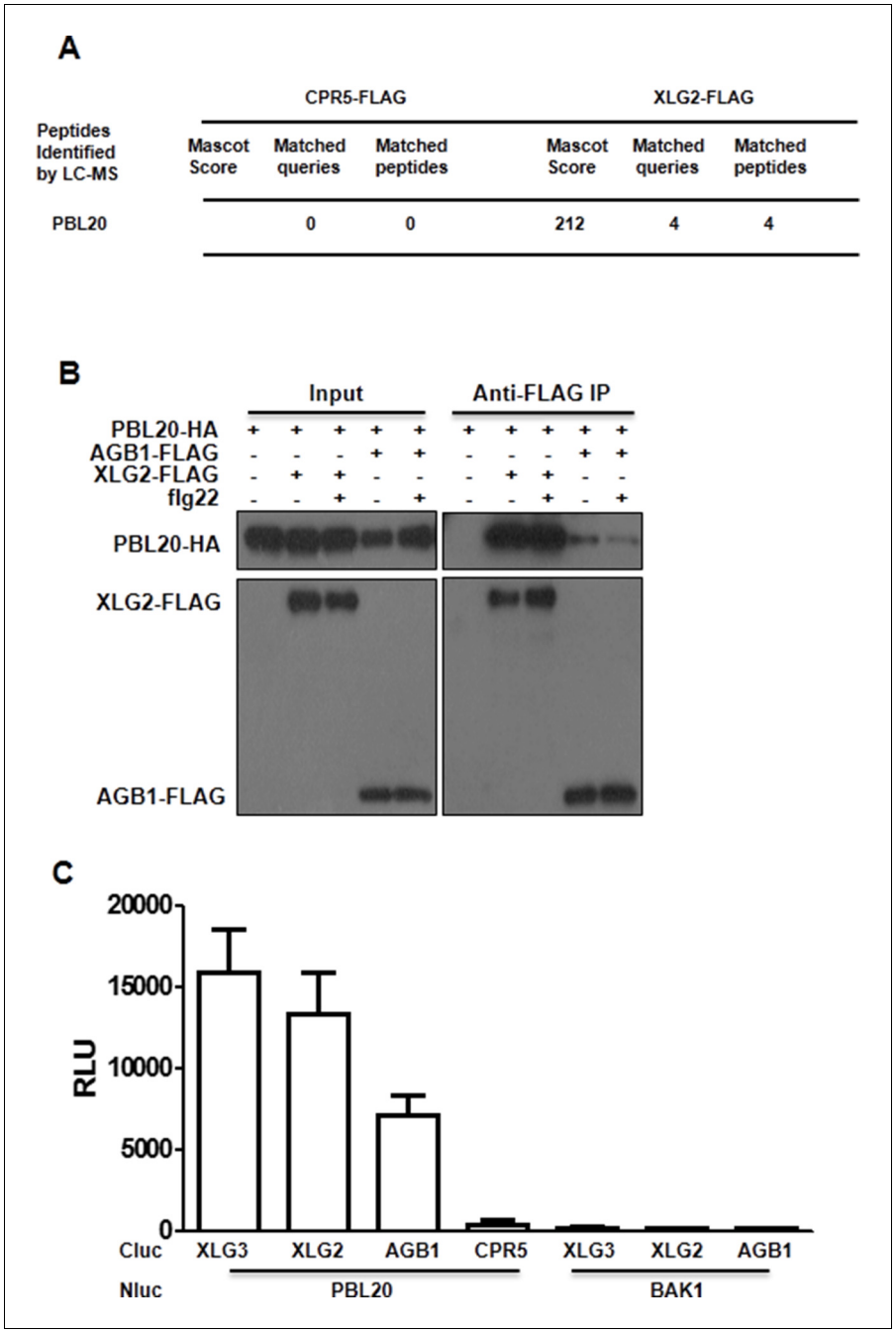

Figure 2—figure supplement 1. PBL20 interacts with G proteins. (**A**) Identification of PBL20 as a XLG2-interacting protein. XLG2-FLAG was expressed in protoplasts, isolated by anti-FLAG immunoprecitation and subject to LC-MS/MS. No PBL20 peptides were identified in the control experiment using CPR5-FLAG as bait. (**B**) PBL20 interacts strongly with XLG2 and weakly with AGB1 in Arabidopsis protoplasts. Co-IP assay was performed using Arabidopsis protoplasts transfected with the indicated constructs. Three independent experiments were performed with similar results. (**C**) PBL20 interacts with XLG2 in *Nb* plants. *Nb* leaves were infiltrated with Agrobacteria containing the indicated constructs and luciferase activity was recorded 2 days later (mean ± SD; n≥6; representative data from two independent experiments are shown).

DOI: 10.7554/eLife.13568.009

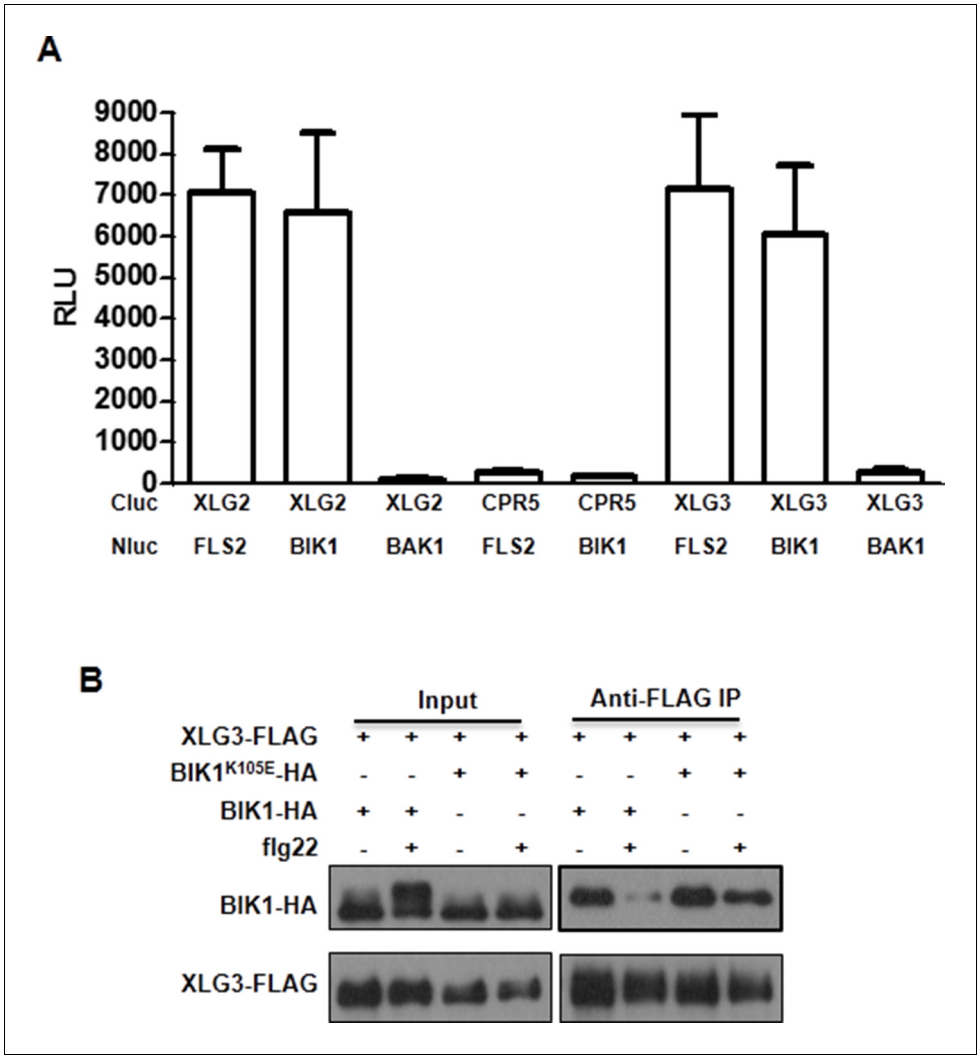

Figure 2—figure supplement 2. XLG3 interacts with BIK1. (**A**) XLG3 interacts with BIK1 in *Nb* plants. Agrobacteria containing the indicated constructs were infiltrated into *Nb* leaves, and luciferase activity was recorded 2 days later (mean ± SD; n ≥ 6). (**B**) XLG3 interacts with BIK1 in protoplasts. Co-IP assay was performed using WT Arabidopsis protoplasts transfected with the indicated constructs. Representative data from three independent experiments are shown.

DOI: 10.7554/eLife.13568.010

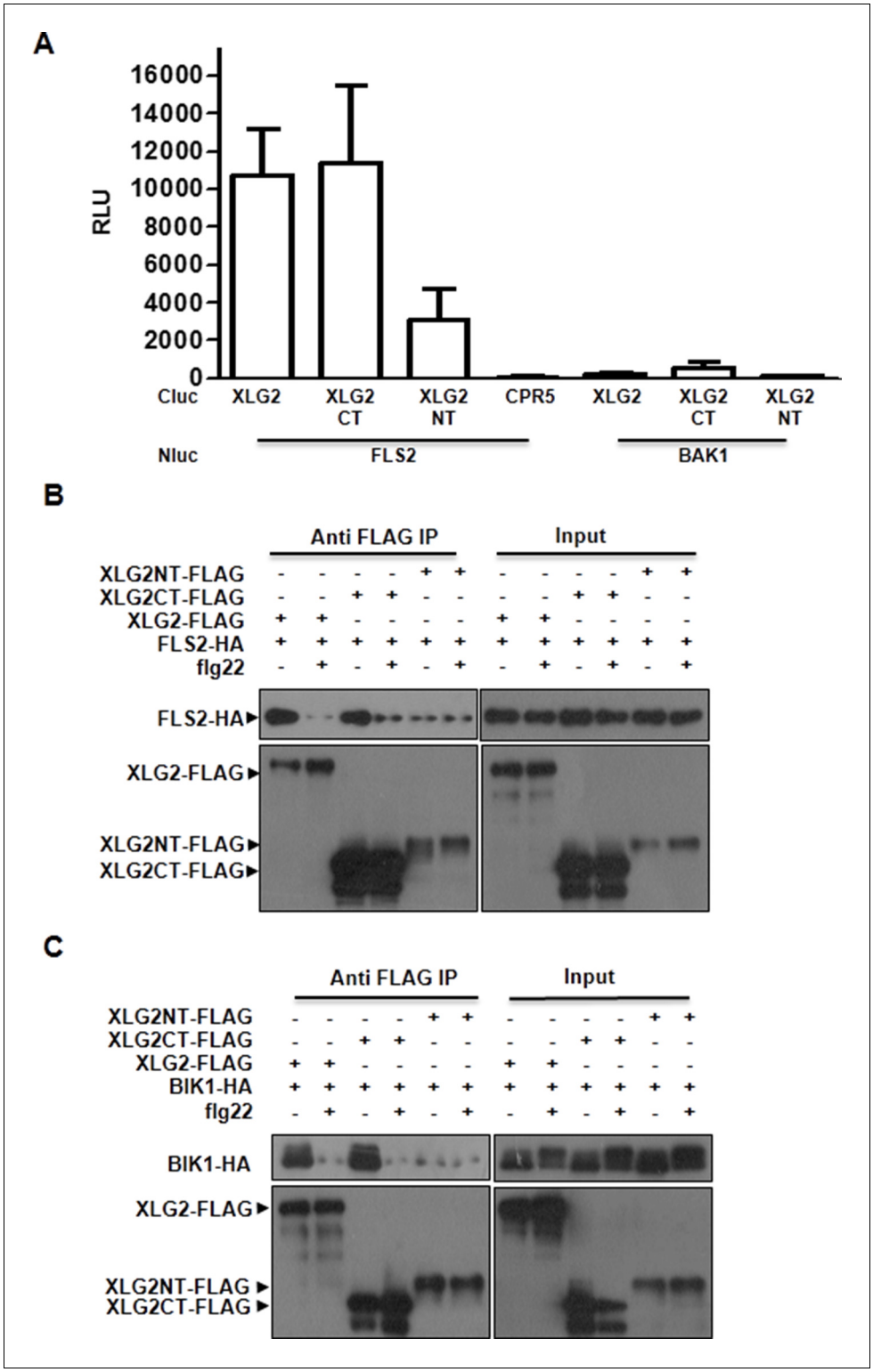

Figure 2—figure supplement 3. XLG2 interacts with FLS2 and BIK1 primarily through the C terminus. (**A**) XLG2 C terminus interacts with FLS2 in *Nb* plants. Agrobacteria carrying the indicated constructs were infiltrated into *Nb* leaves, and luciferase activity was recorded 2 days later (mean ± SD; n≥6). (**B**) XLG2 C terminus interacts with BIK1. (**C**) XLG2 C terminus interacts with FLS2. WT Arabidopsis protoplasts were transfected with the indicated constructs, and total protein was subject to Co-IP assays. Two independent experiments were performed with similar results.

Figure 2—figure supplement 3 continued on next page

Figure 2—figure supplement 3 continued

DOI: 10.7554/eLife.13568.011

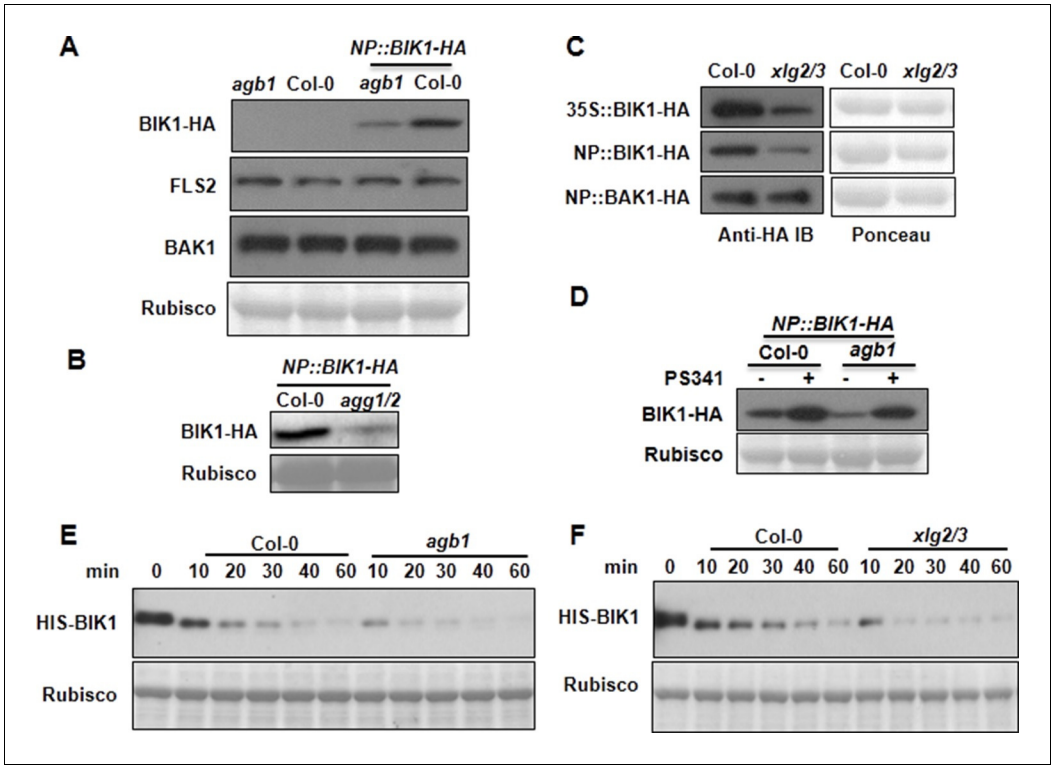

Figure 3. G proteins positively regulate immunity and BIK1 stability. (**A**) *AGB1* is required for accumulation of BIK1, but not FLS2 and BAK1. *BIK1-HA* was introduced into *agb1* by crossing, homozygotes of the indicated genotypes in F3 generation were used for immunoblot analyses. (**B**) *AGG1/2* are required for BIK1 stability. *NP::BIK1-HA* was introduced into *agg1/2* by crossing, homozygous plants in F3 generation were subject to immunoblot analyses. (**C**) *XLG2/3* are required for BIK1 accumulation. NP::BIK1-HA, 35S::BIK1-HA and NP::BAK1-HA plasmids were transiently expressed in WT and *xlg2/3* protoplasts, and accumulation of BIK1 and BAK1 was determined by immunoblot analyses. (**D**) AGB1 regulates BIK1 accumulation through the proteasome pathway. One-week-old *NP::BIK1-HA* seedlings of WT (Col-0) or *agb1* background were pretreated with DMSO (-) or 100 μM proteasome inhibitor PS341(+) for 8 hr before total protein was isolated for immunoblot analysis. (**E**) The *agb1* extract shows accelerated degradation of BIK1 in vitro (**F**) The *xlg2 xlg3* extract shows accelerated degradation of BIK1. Total extracts from WT (Col-0), *agb1* and *xlg2 xlg3* seedlings were incubated with HIS-BIK1 protein at 22°C for the indicated times, and equal amounts of sample were analyzed using anti-HIS immunoblot. Each experiment was repeated at least three times, and data from one representative experiment are shown.
DOI: 10.7554/eLife.13568.012

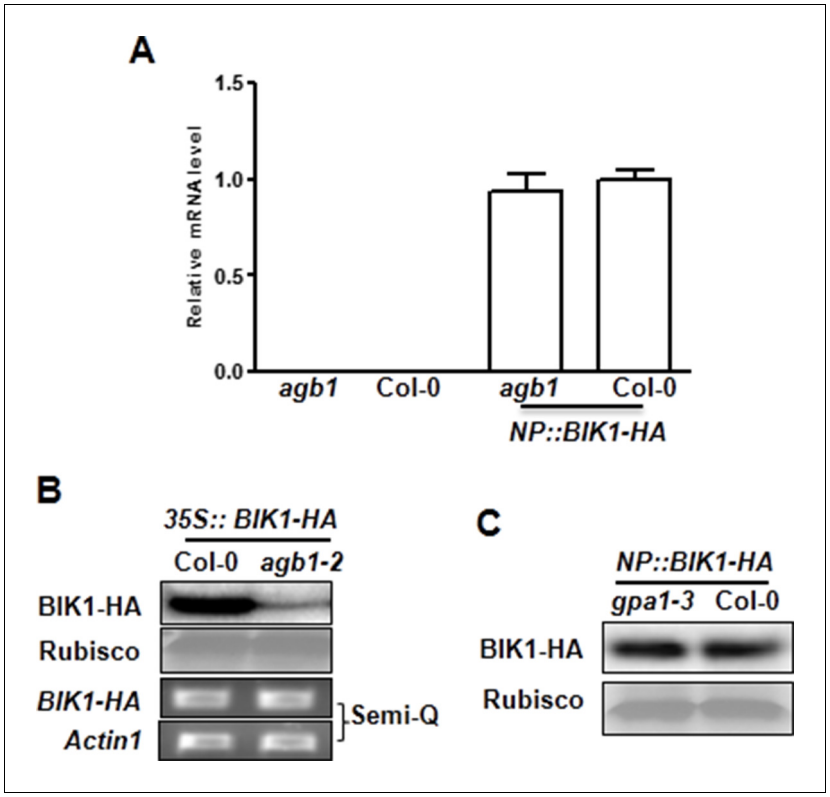

Figure 3—figure supplement 1. G proteins are required for BIK1 stability. (**A**) *agb1* plants are largely normal in *BIK1* transcription. Total RNA was isolated from plants of the indicated genotypes, and quantitative real time PCR was carried out to determine *BIK1-HA* transcript levels. (**B**) Accumulation of BIK1 expressed from a transgene under control of the constitutive 35S promoter was similarly compromised in the *agb1-2* mutant. *35S::BIK1-HA* transgenic lines in WT and *agb1-2* background with similar *BIK1* transcript levels were identified by Semi-qPCR and used for detection of BIK1 accumulation. (**C**) Accumulation of BIK1 is not compromised in the *gpa1-3* mutant. *NP::BIK1-HA* was introduced into *gpa1-3* by crossing, and BIK1 accumulation was detected by anti-HA immunoblot. Three independent experiments were performed with similar results.
DOI: 10.7554/eLife.13568.013

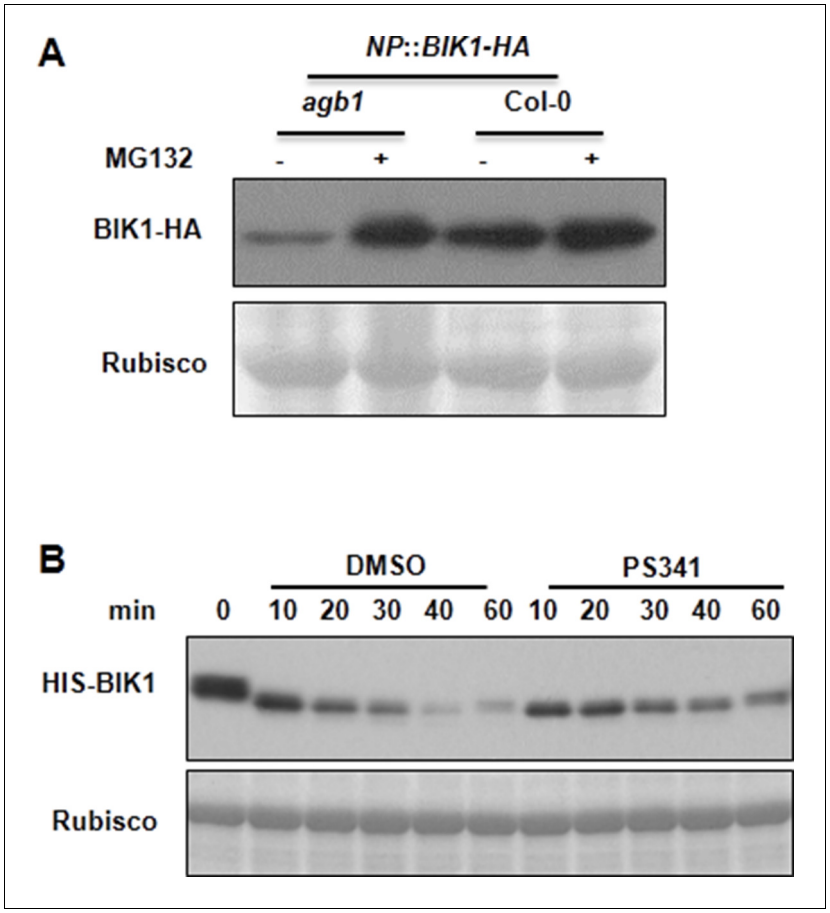

Figure 3—figure supplement 2. AGB1 regulates BIK1 stability through proteasome pathway. (**A**) Treatment with MG132 allows accumulation of BIK1 in *agb1* mutant seedlings. *NP::BIK1-HA* seedlings of WT (*AGB1*) and *agb1* background were treated with DMSO (-) or 100 μM specific proteasome inhibitor MG132 (+) for 8 hr, BIK1 stability was detected by anti-HA immunoblot. (**B**) Treatment with PS341 inhibits BIK1 degradation in vitro. Total extracts from WT plants pretreated with DMSO or 100 μM PS341 were incubated with the HIS-BIK1 recombinant protein, and equal amounts of sample were withdrawn at the indicated times for anti-HIS immunoblot assays. Three independent experiments were performed with similar results.

DOI: 10.7554/eLife.13568.014

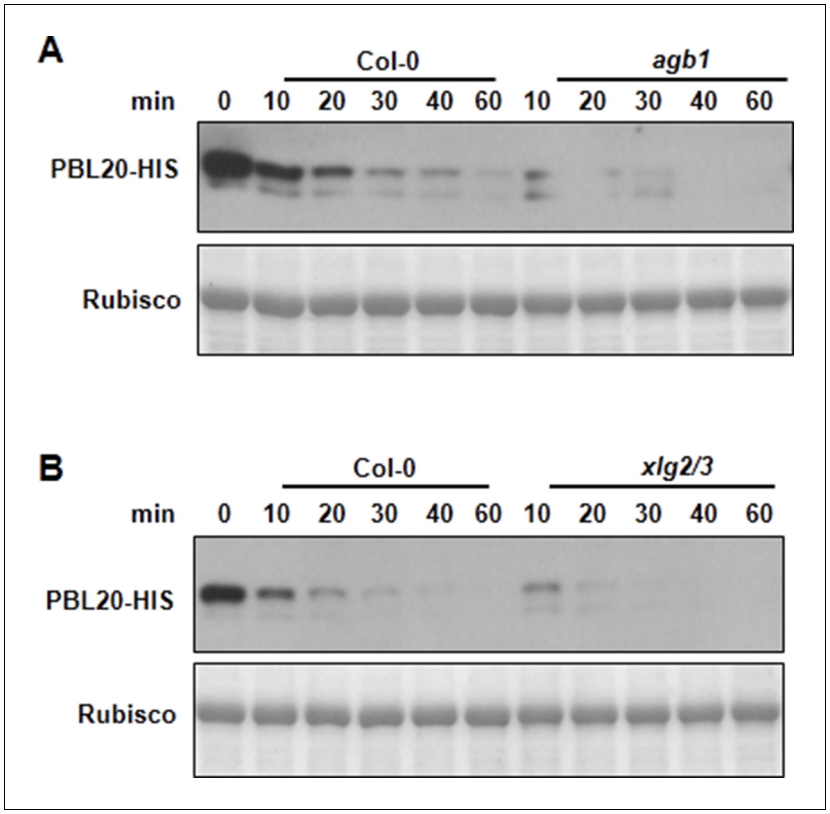

Figure 3—figure supplement 3. *AGB1* and *XLG2/3* attenuate PBL20 degradation. (**A**) Accelerated PBL20 degradation in *agb1* extracts. (**B**) Accelerated PBL20 degradation in *xlg2 xlg3* extracts. Total extracts from WT, *agb1* and *xlg2/3* were incubated with the PBL20-HIS recombinant protein, and equal amounts of sample were withdrawn at the indicated times for anti-HIS immunoblot analyses. Two independent experiments were performed with similar results.

DOI: 10.7554/eLife.13568.015

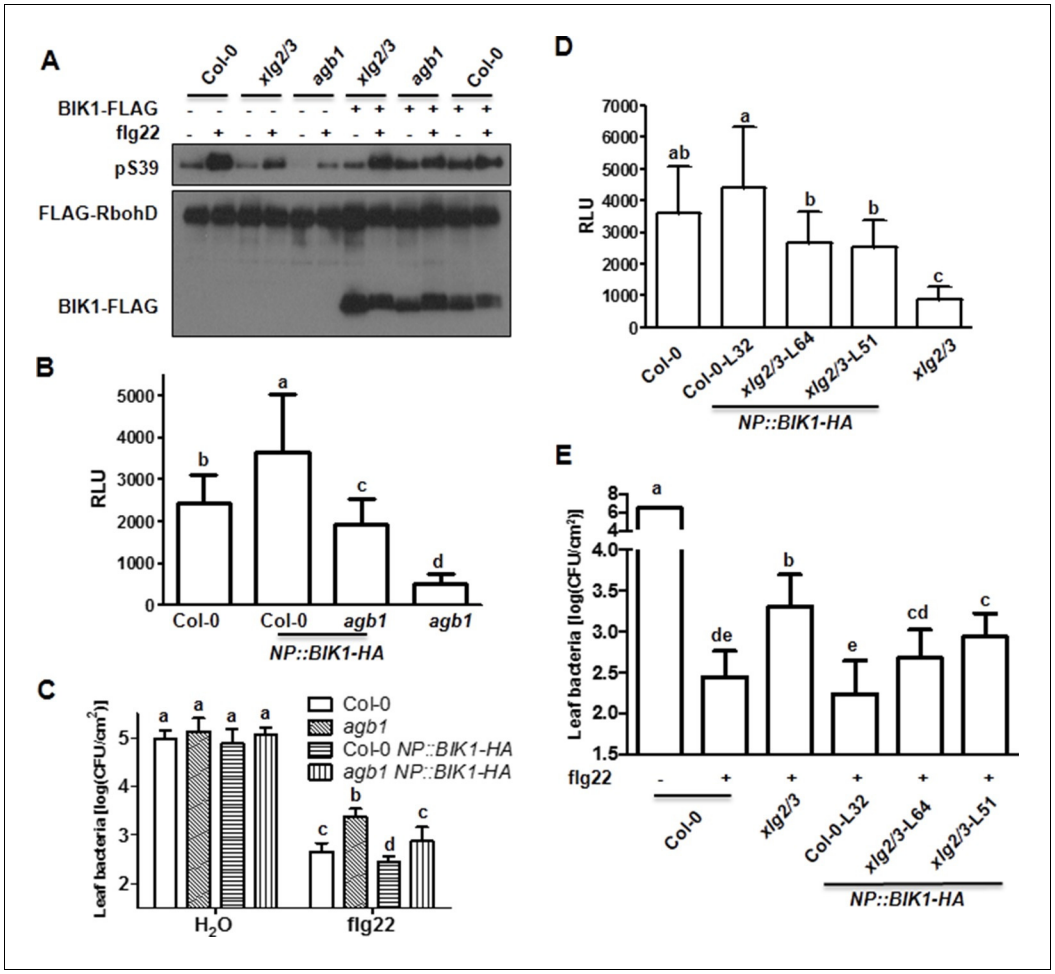

Figure 4. BIK1 level accounts for G protein-mediated regulation of FLS2 immunity. (**A**) Transient expression of BIK1 in *agb1* and *xlg2/3* mutant protoplasts restores RbohD phosphorylation. FLAG-RbohD and BIK1-HA constructs are transiently expressed in protoplasts from WT (Col-0), *agb1* and *xlg2/3*. FLAG-RbohD protein was affinity purified and detected by anti-FLAG and anti-pSer39 immunoblots. (**B**) *BIK1* transgene restores flg22-induced ROS burst in *agb1*. (**C**) *BIK1* transgene partially restores flg22-induced resistance to *Pst* in *agb1*. *NP::BIK1-HA* was introduced into *agb1* by crossing, transgenic lines of *agb1* or Col-0 background in the F3 generation were used for the assays. (**D**) *BIK1* transgene partially restores flg22-induced ROS burst in *xlg2 xlg3* mutant. (**E**) *BIK1* transgene partially restores flg22-induced resistance to *Pst*. The *NP::BIK1-HA* transgene was introduced into WT (Col-0-L32) and *xlg2 xlg3* (*xlg2/3*-L64 and *xlg2/3*-L51) plants by *Agrobacterium*-mediated transformation. Independent T2 transgenic lines were used for the assays. Peak relative luminescence unit (RLU) values were shown for ROS assays (**B** and **D**) and leaf bacterial populations 2 days after bacterial inoculation were shown for flg22-protection assays (**C** and **E**). Bars in B-E represent mean ± SD ($n \geq 6$; $p<0.05$, Student's t-test; different letters indicate significant difference). Each experiment was repeated two (**A**) or three (**B**–**E**) times, and data of one representative experiment are shown.

DOI: 10.7554/eLife.13568.016

The following source data is available for figure 4:

Source data 1. Raw data and exact p value of ***Figure 4B—E***.

DOI: 10.7554/eLife.13568.017

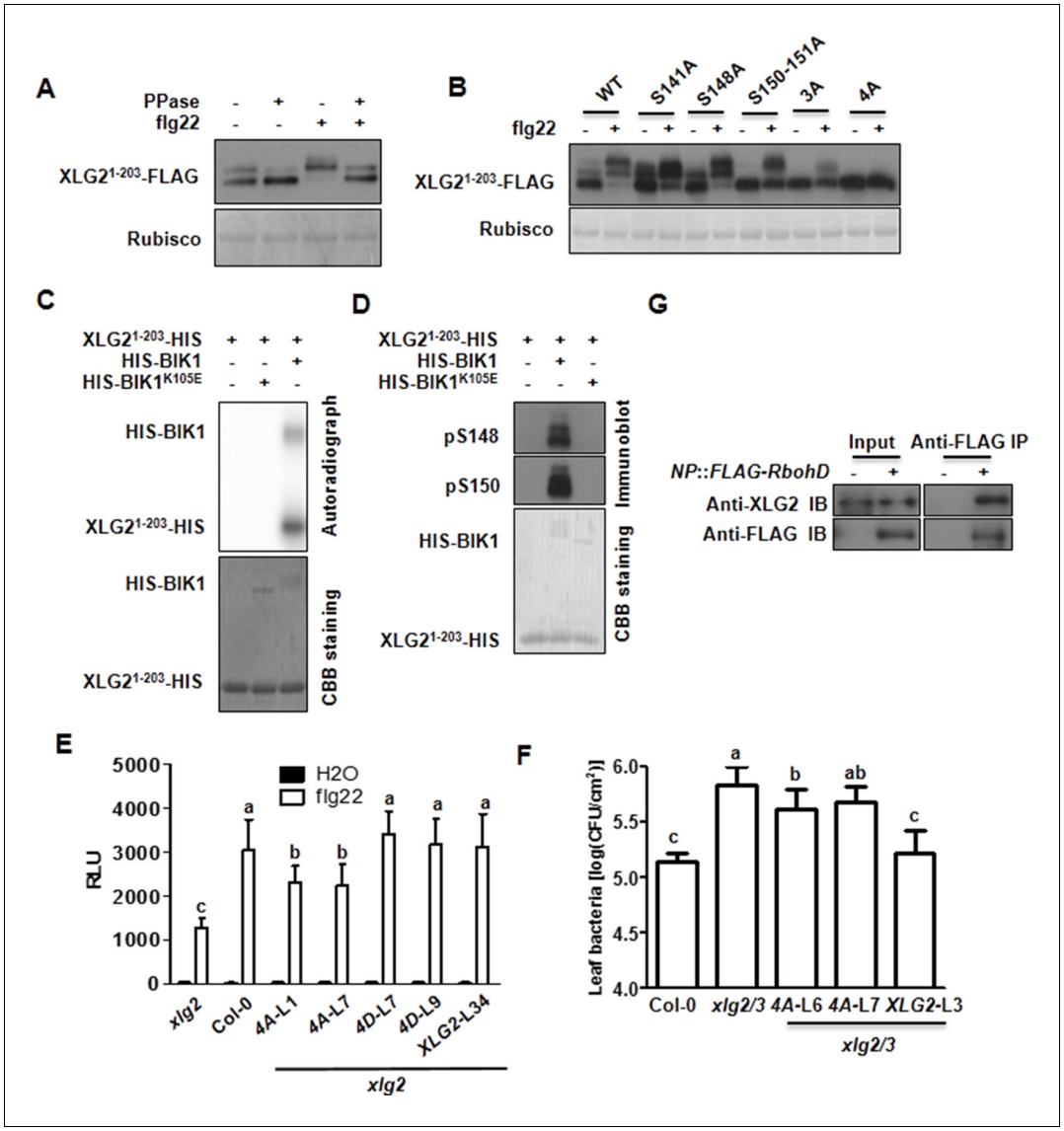

Figure 5. Phosphorylation of XLG2 by BIK1 regulates flg22-induced ROS. (**A**) Flg22-induces phosphorylation of XLG2 in the N terminus. Protoplasts expressing XLG2$^{1-203}$-FLAG were treated with flg22. The total protein was treated with (+) or without (-) λ protein phosphatase (PPase) prior to anti-FLAG immunoblot analysis. (**B**) Flg22-induced phosphorylation of XLG2 in protoplasts primarily occurs in Ser141, Ser148, Ser150 and Ser151. Different mutated form of XLG2$^{1-203}$-FLAG constructs were transiently expressed in WT protoplast, treated with flg22 and the migration of XLG2$^{1-203}$-FLAG were examined by anti-FLAG immunoblot. (**C**) BIK1 phosphorylates XLG2 N terminus in vitro. XLG2$^{1-203}$-HIS was incubated with HIS-BIK1 and HIS-BIK1^{K105E} in the presence of ^{32}P-γ-ATP and analyzed by autoradiography. CBB, coomassie brilliant blue. (**D**) BIK1 phosphorylates XLG2 at Ser148 and Ser150 in vitro. XLG2$^{1-203}$-HIS was incubated with HIS-BIK1 and HIS-BIK1^{K105E} in kinase reaction buffer. Protein phosphorylation was detected by anti-pSer148 and pSer150 immunoblots. (**E**) XLG2 phosphorylation is required for flg22-induced ROS. *xlg2* mutant plants were transformed with WT (*NP::XLG2*-L34), non-phosphorylatable (4A-L1 and 4A-L7), or phospho-mimicking (4D-L7 and 4D-L9) forms of *XLG2* under control of the native *XLG2* promoter. Independent T2 lines were examined for flg22-induced ROS burst and peak relative luminescence unit (RLU) values are shown. (mean ± SD; n ≥ 6; p<0.05, Student's t-test; different letters indicate significant difference). (**F**) XLG2 phosphorylation is required for *Pst* resistance. *xlg2/3* double mutant plants were transformed with WT (*XLG2*-L3) or non-phosphorylatable (4A-L6 and 4A-L7) form of *XLG2* under control of the native *XLG2* promoter. Independent T2 lines were inoculated with *Pst*, and bacterial populations in leaves were measured 3 days post inoculation. (mean ± SD; n ≥ 6; p<0.05, Student's t-test; different letters indicate significant difference). (**G**) XLG2 interacts with RbohD in Arabidopsis plants. *rbohD* plants were transformed with the *FLAG-RbohD* transgene

Figure 5 continued on next page

Figure 5 continued

under control of the *RbohD* native promoter. The resulting plants were used for Co-IP assay. Each experiment was repeated two (**C**, **G**) or three (**A**, **B**, **D–F**) times, and data of one representative experiment are shown.

DOI: 10.7554/eLife.13568.018

The following source data is available for figure 5:

Source data 1. Raw data and exact p value of ***Figure 5E*** and ***F***.

DOI: 10.7554/eLife.13568.019

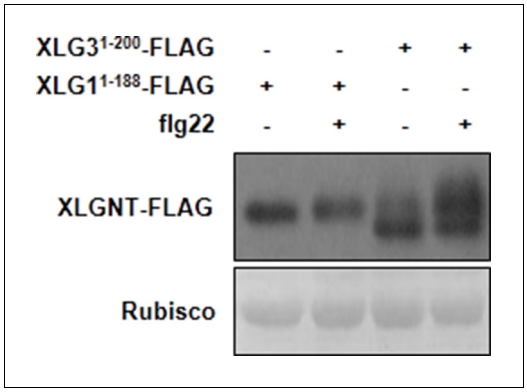

Figure 5—figure supplement 1. The N terminus of XLG3, but not XLG1, is phophorylated upon flg22-treatment. WT protoplasts were transfected with XLG1$^{1-188}$-FLAG or XLG3$^{1-200}$-FLAG, treated with flg22, and protein was analyzed by anti-FLAG immunoblot.
DOI: 10.7554/eLife.13568.020

Phospho-peptide sequence	Position	Phospho-peptide sequence	Position
KLLPFPpSPNPK	S13	SPADFRLSPpSSPLSASAR	S150
LLPFPpSPNPK	S13	SPADFRLpSPp(SS)PLSASAR	S148 S150/151
RDNREpSDDDDETSSGYR	S23	SPADFRLSPpSpSPLpSASAR	S150 S151 S154
DNREpSDDDDETSSGYR	S23	LSPp(SS)PLSASAR	S150/151
ALPVEVDQIPTALPVpSFSSLR	S69	Lpp(SPSSPLSAS)AR	S148/150/151/154/156
ALPVEVDQIPTALPVSFp(SS)LR	S71/72	LSPSSPLSApSAREEDHLDDDR	S156
DVVSGp(SSSSSSS)K	S(124-130)	Lpp(SPSSPLSAS)AREEDHLDDDRVSDVGPR	S148/150/151/154/156
DVVSGp(SSSSSSS)KR	S(124-130)	EEDHLDDDRVpSDVGPR	S169
DVVSGpp(SSSSSSS)KRLDVPEEVK	S(124-130)	FVEPFQSSECDESSYVpSDGESIAATHR	S194
RLDVPEEVKpSPADFR	S141	FVEPFQSSECDESpSYVSDGESIAATHR	S191
LDVPEEVKpSPADFR	S141	QSSECDESSYVpSDGESIAATHR	S194
SPADFRLpSPSSPLSASAR	S148	SLYNVpSFSLEDR	S488
		TCEWFEDFNPLISQNQp(TS)R	T773/S774

Figure 5—figure supplement 2. Phospho-sites in XLG2 isolated from flg22-treated protoplasts. List of phospho-peptides identified. Protoplasts prepared from WT plants were transfected with XLG2-FLAG and treated with flg22 for 10 min, affinity-purified and subjected to LC-MS/MS for phospho-sites identification.

DOI: 10.7554/eLife.13568.021

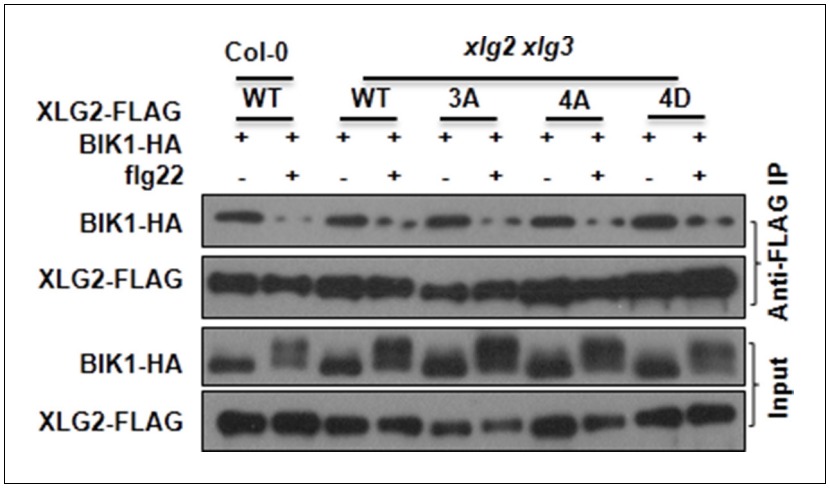

Figure 5—figure supplement 3. Mutations that block or mimic XLG2 phosphorylation do not impact BIK1 stability and XLG2-BIK1 interaction. WT or *xlg2 xlg3* protoplasts were transfected with BIK1-HA along with WT, non-phosphorylatable (3A, 4A), phospho-mimicking (4D) forms of XLG2-FLAG constructs, treated with (+) or without (-) flg22, and total protein was subject to Co-IP assays and immunoblot analysis. Three independent experiments were performed with similar results.

DOI: 10.7554/eLife.13568.022

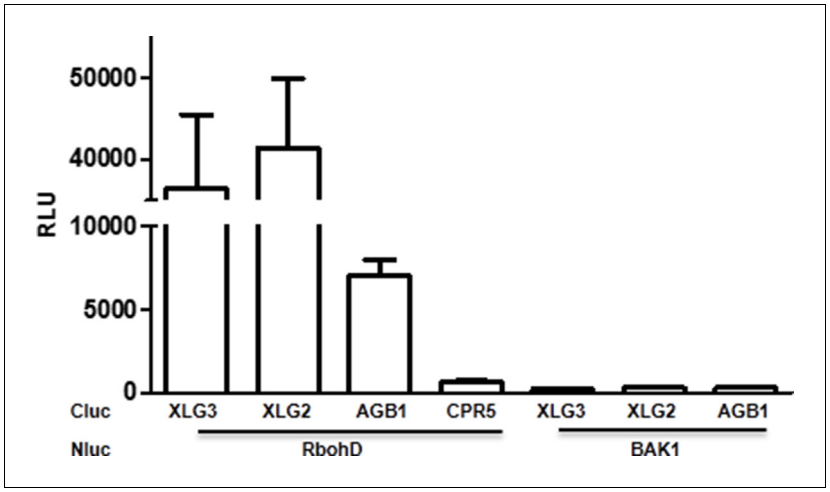

Figure 5—figure supplement 4. XLG2/3 interact with RbohD in Nb plants. Agrobacteria containing the indicated constructs were infiltrated in to *Nb* leaves, and luciferase activity was recorded 2 days later (mean ± SD; n≥6; representative data from 2 independent experiments are shown).
DOI: 10.7554/eLife.13568.023

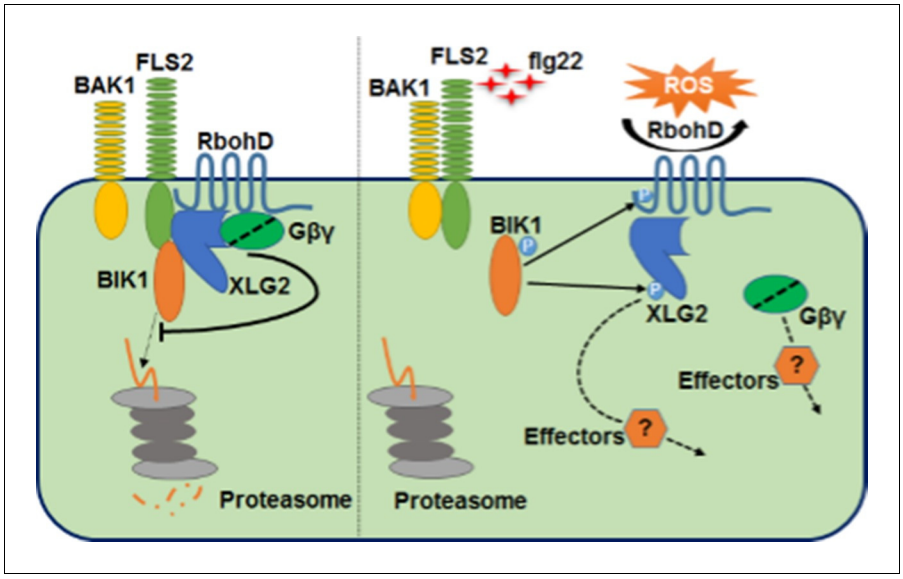

Figure 6. Model for G protein-coupled FLS2 signaling. In the pre-activation state, the heterotrimeric G proteins composed of XLG2/3, AGB1, and AGG1/2 interact with the FLS2-BIK1 complex. Stimulation by flg22 induces BAK1-FLS2 interaction and activation of the receptor complex. This leads to the activation of the G proteins and phosphorylation of XLG2 in the N terminus. The activated G proteins dissociate from the receptor complex and regulate RbohD and other downstream effectors to positively modulate immune responses.
DOI: 10.7554/eLife.13568.024